

Received December 21, 2019, accepted December 30, 2019, date of publication January 3, 2020, date of current version January 9, 2020.

Digital Object Identifier 10.1109/ACCESS.2019.2963692

Distributed Optimal Vehicle-To-Grid Approaches With Consideration of Battery Degradation Cost Under Real-Time Pricing

KENECHUKWU GINIGEME^{ID} AND ZHANLE WANG^{ID}, (Member, IEEE)

Electronic Systems Engineering, University of Regina, Regina, SK S4S 0A2, Canada

Corresponding author: Zhanle Wang (zhanle.wang@uregina.ca)

This work was supported by the University of Regina through the Faculty Research Grant and NSERC Cohort Program.

ABSTRACT Electric vehicles (EV) are becoming increasingly popular due to their efficiency and potentials to reduce greenhouse gas emission. However, penetration of a very large number of EVs can have negative impacts on power systems. This study proposes optimal vehicle-to-grid (V2G) models to incorporate the EV penetration by minimizing multiple objectives including the peak demand, the variance of load profile, the battery degradation cost and the EV charging/discharging cost based on real-time pricing (RTP). The proposed models incorporate EV driving patterns including driving distance, driving periods, and charging/discharging levels and locations. A nonlinear battery degradation cost function is linearized and incorporated into the optimal models. In addition, a distributed control algorithm is developed to implement the optimal models. One-day simulation results show that the proposed approach can reduce the peak demand and the variance of the load profile by 7.8% and 81.9%, which can significantly improve power system stability and energy efficiency. In addition, the sum of EV charging/discharging cost and battery degradation cost is decreased from \$251 to -\$153. In fact, 100 EVs earn \$153 in the day from the V2G program. The approaches can be used by a load aggregator or a utility to effectively incorporate EV penetration to power systems to unlock V2G opportunities and mitigate negative impacts.

INDEX TERMS Electric vehicles, vehicle-to-grid, battery degradation, real-time pricing, convex optimization, demand response.

NOMENCLATURE

VARIABLES AND FUNCTIONS

α	decay coefficient	$max(\cdot)$	peak demand of the load profile
β	constant in Eq. 6	P_{rated}	rated EV charging/discharging power
σ	standard deviation	SOC_{min}	minimum SOC
μ	average value	SOC_{max}	maximum SOC
λ, ν, κ	coefficients for weighted average	SOC_{acc}	accepted SOC before driving EV
\mathcal{T}	time horizon	$P_{base,t}$	base load at time t
a_1, a_2, b_1, b_2	constants in Eq. 3	P_t^{EV-i}	EVs except the i^{th} EV
C_b	battery cost per kWh	i	index of EV
C_L	battery life cycle	LC	labor cost of replacing a battery
$DC(DOD)$	degradation cost	L_0	cycle life at 100% of DOD
DOD	depth of discharge	$P_t^{EV_i}$	electricity load of the i^{th} EV
E_0	rated battery capacity	RTP_t	real time price at time t
EV_i	the i^{th} EV	SOC	state of charge
		t	time
		t_1	home leaving time
		t_2	work arrival time
		t_3	work leaving time
		t_4	home arrival time
		$var(\cdot)$	variance of the load profile

The associate editor coordinating the review of this manuscript and approving it for publication was Salvatore Favuzza^{ID}.

ACRONYMS

DR	demand response
EV	electric vehicle
LMP	locational marginal price
RTP	real-time pricing
V2H	vehicle-to-home
V2G	vehicle-to-grid
V2V	vehicle-to-vehicle

I. INTRODUCTION

V2G features with bi-directional power flow and two-way communication, which allows EVs act as both controllable loads under demand response (DR) and distributed energy resources [1], [2]. The number of EVs is expected to reach 5.1 million globally by 2020 [3]. On one hand, EV penetration and uncontrolled EV charging can dramatically increase peak demand and have negative impacts on the power system [4], [5]. On the other hand, EVs have batteries with a significant energy capacity and are parked 95% of time in average [6], [7], which can - through V2G applications - provide ancillary services such as peak demand shaving, frequency regulation, voltage regulation and renewable energy integration [8]–[12].

Various frameworks, modeling, and optimization approaches have been developed to facilitate V2G applications. The frameworks can be summarized from small scale to large scale as: vehicle-to-home (V2H), vehicle-to-vehicle (V2V) and V2G [1]. Under the framework of V2H, an optimal home energy management system was developed to coordinate various household loads, photovoltaics and EVs by minimizing overall energy cost under energy price tag [13]. Since household loads cannot be modeled deterministically, a layered stochastic approach was developed to minimize household electrical cost under RTP and incentives, which considers EVs as controllable loads [14]. In a larger scale residential sector, a stochastic optimization model was developed to minimize the power loss through coordination of EV charging in a residential distribution grid [15].

Under the framework of V2V, a localized peer-to-peer electricity trading among EVs was developed for DR applications in balancing local electricity demand out of self-interests smart grids [16]. Similarly, EVs were modeled as self-interested agents in a multi-agent system for a DR application in an electricity market [17]. To coordinate EV charging under DR in parking stations, a real-time control scheme was proposed in [18]. In V2G framework, smart charging strategies were developed for optimal EV integration to distribution systems, and the model was tested in a 37-bus distribution system [19]. The work in [20] developed an optimal dispatching model with multiple objectives to coordinate charging/discharging of a very large number of EVs in microgrids

However, the above-mentioned research did not consider batter degradation. The battery is one of the most important and expensive components in EVs [21] and V2G applications requires frequent EV charging and/or discharging.

The charging/discharging is associated with a gradual change in the physical structure of both the electrolyte and electrode, which causes battery degradation [22]. Therefore, the batter degradation should be studied and considered in V2G programs.

Modeling EV battery degradation can be burdensome and computationally complex since many factors account for the battery ageing process [22]. Extensive efforts have been made to understand the battery degradation for lithium ion battery [23]. Consequently, various capacity loss models have been established based on different aging mechanisms such as solid electrolyte interphase formation [24], parasitic side reaction [25] and resistance increase [26].

As one of the examples, the degradation cost can be estimated as follows [27], [28].

$$DC = k \frac{C_b E_0 + LC}{C_L E_0 DOD} \quad (1)$$

where DC is the degradation cost for each charging/ discharging cycle. k is a constant value. C_b is the battery cost per kWh , E_0 is the rated battery capacity and LC is labor cost of replacing a battery. DOD is depth of discharge, and $DOD = 1 - SOC$, where SOC represents state of charge. C_L is the life cycle of a battery, which is shown in Eq. 2.

The battery cycle life C_L depends on the DOD of each charging/discharging cycle. For example, a lower DOD can lead to higher battery life cycles not only because it represents less energy of charging/discharging, but also it results in lower degradation cost. Typically, 20% of final DOD is recommended for a Li-Ion battery [26]. Eq. 2 shows the cycle life as a function of DOD based on experiment of Saft Li-Ion battery [28].

$$C_L = L_0 e^{\alpha(1-DOD)} \quad (2)$$

where L_0 is the cycle life at 100% of DOD . α is the decay coefficient. Typically, α falls between values of 3 and 6 for different batteries and the maximum cycle life is usually at a $DOD = 1/\alpha$. The Saft Li-Ion experiment show 3000 cycles at a DOD of 100% and 1,000,000 cycles at a DOD of 3% [29]. In addition, experiments ($\alpha = 6$) showed that the most economical DOD ranged between 16.7% and 33.3% [26].

Recently, various battery degradation cost functions have been incorporated into optimal approaches. For instance, an EV charge/discharge optimization model with consideration of the battery degradation cost was developed for frequency regulation [30]. An optimization model is also proposed to minimize both battery charging/discharging cost and battery degradation cost based on three-phase power flow and sensitivity approaches [31]. An optimization problem was formulated in [32], in which the cost function is the combination of electricity prices and the battery degradation cost. However, these studies did not consider the EV driving patterns such as driving distance, driving times, and EV charging/discharging levels and locations.

In our study, we developed two optimal V2G models for EV penetration into a microgrid. Multiple objectives were

proposed to minimize the peak demand, the variance of load profile, the battery degradation cost and the EV charging/discharging cost based on RTP. A linearized degradation cost function was developed.

The vehicle driving patterns was incorporated and the level-1 charging/discharging at homes and level-2 charging/discharging at workplaces were considered. The contributions of this work are summarized as follows.

1. Two optimal V2G approaches are developed to minimize multiple objectives including the peak demand, the variance of load profile, the battery degradation cost and the charging/discharging cost based on RTP.
2. Weighting factors of the multiple objectives are quantitatively evaluated, and the values can provide a baseline for a utility or an EV aggregator to implement the proposed models.
3. A distributed control algorithm is developed to implement the proposed optimal approaches, which is linearly scalable to control a very large number of EV charging/discharging.
4. Case studies are conducted using the actual data from the (Pennsylvania, Jersey and Maryland) PJM electricity market. Simulation results demonstrate the effectiveness of the proposed approach. More specifically, the peak demand and variance of the load profile is reduced by 7.8% and 81.9%, which can significantly improve the power system stability and reduce the power generation cost. In addition, one EV can earn \$1.5/day in average by using the proposed method.

The rest of the paper is organized as follows. Section II illustrates the methodology. Section III shows the case studies and simulation results followed by a discussion in Section IV. The study is concluded in Section V.

II. METHODOLOGY

A. SYSTEM ARCHITECTURE

In this study, we consider a microgrid having all the three sectors of the power system: residential, commercial and industrial. We focus on the study of EV charging/discharging control and its impact on power systems. Fig. 1 shows the system diagram, where solid lines represent power distribution while dash lines represent communication.

We assume that an EV aggregator is presented and controls EV charging/discharging. We also assume the EVs have information and communication devices installed, and the owners are contracted with the aggregator.

In this study, we optimize EV charging/discharging in a distribution network. The EVs can be charged/discharged at home with level-1 charging stations and at workplace with level-2 charging stations. The daily EV driving distance and driving periods are also considered, which results various battery SOC's.

B. LINEARIZED DEGRADATION COST MODEL

In this study, we linearize the battery degradation cost model shown in Eq. 1 and Eq. 2 by applying the linear regression

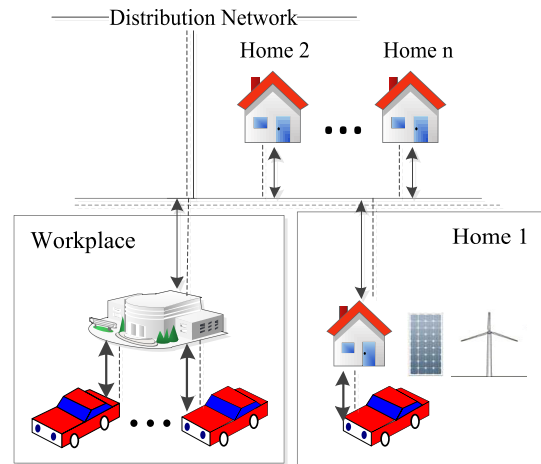


FIGURE 1. System diagram.

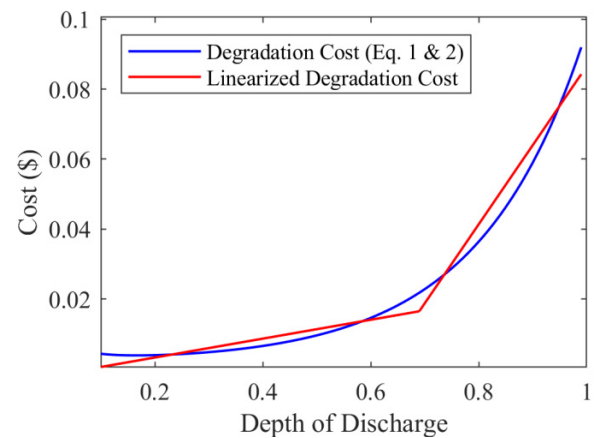


FIGURE 2. Degradation cost.

approach. The linearized degradation cost model is shown in Eq. 3.

$$DC(DOD) = \begin{cases} a_1 \times DOD - b_1, & \forall 0 \leq DOD \leq 70\% \\ a_2 \times DOD - b_2, & \forall 70\% < DOD \leq 100\% \end{cases} \quad (3)$$

where a_1, a_2, b_1, b_2 are constants.

The blue line in Fig. 2 shows the actual battery degradation cost based on Eq. 1 and Eq. 2, and the red line shows the battery degradation cost based on the proposed linearized degradation cost model. To calculate a_1, a_2, b_1, b_2 , we first generated a set of data using Eq. 1 and Eq. 2, and then used Eq. 3 to fit the data by the linear regression method.

We incorporate the linearized degradation cost model into optimal V2G models.

C. OPTIMAL V2G MODELS

In this section, we discuss two optimal V2G models. Model 1 is to minimize the peak demand of the load profile and the battery degradation cost. Model 2 minimizes the variance of

the load profile, the battery degradation cost and the charging/discharging cost based on RTP.

Model 1

$$\begin{aligned} \text{minimize } \max_{P_t^{EV_i}} & \left(P_t^{EV_i} - P_{t \in [t_1, t_2] \cup [t_3, t_4]}^{EV_i} \right. \\ & \left. + P_t^{EV_{-i}} + P_{base,t} \right) + \lambda \sum_{t \in \mathcal{T}} DC(DOD_t) \left| P_t^{EV_i} \right| \end{aligned} \quad (4)$$

subject to

$$-P_{rated} \leq P_t^{EV_i} \leq P_{rated}, \forall t \in [t_2, t_3] \cup [t_4, t_1] \quad (5)$$

$$\sum_t P_t^{EV_i} = \beta E_0, \forall t \in [t_1, t_2] \cup [t_3, t_4] \quad (6)$$

$$SOC_t = SOC_0 + \sum_{i=0}^t P_t^{EV_i} \quad (7)$$

$$SOC_{min} \leq SOC_t \leq SOC_{max}, \quad \forall t \in \mathcal{T} \quad (8)$$

$$SOC_{t_2} \geq SOC_{acc} \quad (9)$$

$$SOC_{t_4} \geq SOC_{acc} \quad (10)$$

$$DOD_t = 1 - SOC_t, \quad \forall t \in \mathcal{T} \quad (11)$$

The optimization model is comprised of two objectives. The first term, $\max(\cdot)$, is the peak demand of the load profile. i is the EV index and EV_i is the i^{th} EV. $P_t^{EV_i}$ is the electricity load at t of the EV_i under optimization.

$P_{t \in [t_1, t_2] \cup [t_3, t_4]}^{EV_i}$ is the power consumption (battery discharging) during EV driving. $t \in [t_1, t_2] \cup [t_3, t_4]$ is the driving period. The energy consumption is constrained by Eq. 6, in which $\beta \leq 1$ is a constant, E_0 is the rated battery capacity, and βE_0 represents the energy consumption of driving an EV. The value of β is discussed in Section III.A.

$P_{t \in [t_1, t_2] \cup [t_3, t_4]}^{EV_i}$ will be negative (constrained by Eq. 6) and uncontrollable. However, this consumption is not the discharging to the power system; therefore, we need to cancel these values by subtracting them from load profile ($P_t^{EV_i} - P_{t \in [t_1, t_2] \cup [t_3, t_4]}^{EV_i}$) in the objective function.

$P_t^{EV_{-i}}$ is the aggregated charging/discharging profiles of the other EVs at time t , which is obtained from information exchange among EVs. $P_{base,t}$ represents the base load at time t . We used the load profile from PJM [33] as the based load and we also called it the load profile without EV charging/discharging. \mathcal{T} is the time horizon.

The second term in the objective function represents the battery degradation cost from EV charging/discharging. $DC(DOD_t)$ is the degradation cost based on the DOD at time t , which is defined in Eq. 3. λ is a non-negative constant to determine the weighted average of peak demand and battery degradation cost. λ also converts the last term to have the same unit as the first term.

Fig. 3 shows the important times, where blue areas show plug-in time while green areas show driving periods. t_1 is the home leaving time and t_2 is the work arrival time. t_3 is the work leaving time and t_4 is the home arrival time. t_1, t_2, t_3

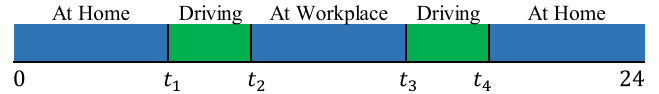


FIGURE 3. Diagram for important times.

and t_4 are assumed to be normally distributed as follows.

$$f(t|\mu, \sigma) = \frac{1}{\sigma \sqrt{2\pi}} e^{-\frac{(x-\mu)^2}{2\sigma^2}} \quad (12)$$

where μ is the average value and σ is the standard deviation.

Eq. 5 describes EV charging/discharging - when plug-in to the power system - cannot exceed the rated power. Eq. 6 shows the power consumption from EV driving.

Eq. 7 calculates the SOC_t , where SOC_0 is the initial SOC. In addition, at any time, the SOC_t should be between the minimum and maximum SOC, e.g., 0% and 100%, which is shown in Eq. 8.

Eq. 9 and Eq. 10 constraint the SOC at t_2, t_4 , the start of driving periods. SOC_{acc} is the accepted SOC before driving the EV so that the driving distance can be fulfilled. The SOC should be greater than a certain accepted value so that it can satisfy a driving range. For example, we use $SOC_{acc} = 50\%$ in this study. Eq. 11 shows DOD of the EV battery.

This model is a convex optimization model since the objective function is convex and all the constraints are affine. More specifically, the first term of the objective function is linear or can be transferred as a linear function by introducing slack variables. In the second term of the objective function, $DC(DOD_t)$ is a piecewise linear function of $P_t^{EV_i}$ and monotonically increases. In addition, λ is non-negative. Therefore, the second term is convex. The objective function is a linear function plus a convex function and therefore is a convex function. In addition, all the constraints are affine functions. Therefore, the optimization model is a convex optimization model and can be solved efficiently.

Model 2

$$\begin{aligned} \text{minimize } \text{var}_{P_t^{EV_i}} & \left(P_t^{EV_i} - P_{t \in [t_1, t_2] \cup [t_3, t_4]}^{EV_i} + P_t^{EV_{-i}} + P_{base,t} \right) \\ & + \nu \sum_{t \in \mathcal{T}} DC(DOD_t) \left| P_t^{EV_i} \right| + \kappa \sum_{t \in \mathcal{T}} RTP_t P_t^{EV_i} \end{aligned} \quad (13)$$

subject to Eq.5 – 11.

Model 2 minimizes the variance of the load profile, the battery degradation cost and the charging/discharging cost based on RTP. In the objective function, $\text{var}(\cdot)$ represents the variance of the load profile, and the second term is the battery degradation cost. The third term is the EV charging/discharging cost, where RTP_t is the real-time price at time t . ν and κ are non-negative constants to determine the weighted average of the three terms. ν and κ also convert the last two terms to have the same unit as the first term.

The first term in the objective function is a quadratic function and both the second term and the third term are linear functions. As illustrated earlier in the Model 1, all the

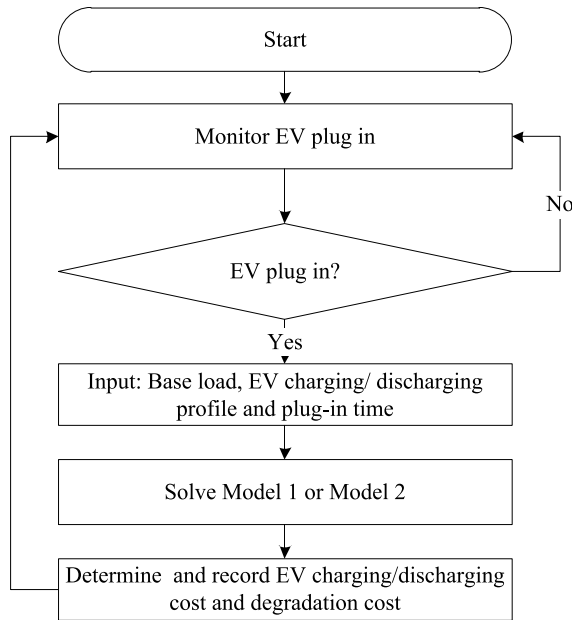


FIGURE 4. The flowchart of the optimal control algorithm.

constraints are affine functions. Therefore, the Model 2 is also a convex optimization model.

D. DISTRIBUTED ALGORITHM FOR OPTIMAL EV MODELS

To implement the proposed optimal V2G models, a distributed control algorithm is designed, and the flowchart is shown in Fig. 4. The EV aggregator monitors if a contracted EV is plugged into the system. If no EVs is plugged in, the system will continuously monitor the action. Otherwise, the proposed Model 1 or Model 2 will be solved based on the input information. The EV charging/ discharging cost and degradation cost will then be determined and recorded.

III. CASE STUDIES

This section presents case studies in the following five scenarios.

Scenario # 1: Without V2G models. No EV charging/ discharging are controlled;

Scenario # 2: Model 1 is applied to only minimize the peak demand ($\lambda = 0$);

Scenario # 3: Model 1 is applied to minimize both the peak demand and the degradation cost;

Scenario # 4: Model 2 is applied to only minimize the variance of the load profile ($\nu = 0, \kappa = 0$);

Scenario # 5: Model 2 is applied to minimize multiple objectives including the variance of the load profile and the degradation cost and the EV charging/discharging cost based on RTP.

A. EXPERIMENTAL SETUP

We assumed that the distribution network has 500 homes. We now discuss the magnitude of power and electricity price of this distribution network in this study. The average

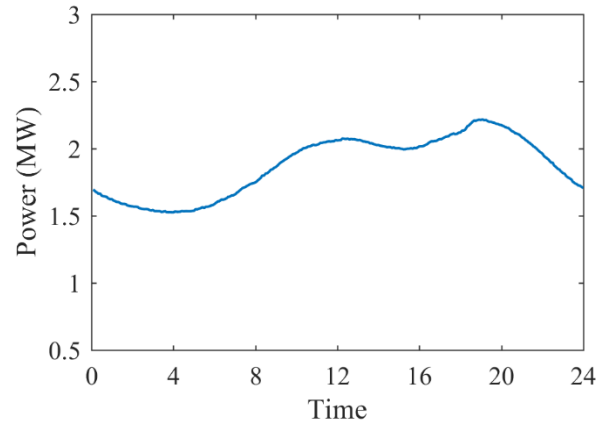


FIGURE 5. The scaled load profile on October 27, 2019 [33]. Used as the base load or load profile without EV penetration.

household electricity usage is approximately 30 kWh per day [34]. In addition, residential customers consume about 1/3 of total electricity [35], [36].

Then, the electricity energy per day in the distribution network including residential commercial and industrial sectors can be calculated as $30 kWh * 500 * 3 = 45 MWh$. To simulate the base load or the load profile without EV penetration, we used the load consumption on October 27, 2019 in the PJM market [33]. This load profile is the aggregated load in the whole service area of the PJM, which is much greater than the load magnitude in this study. Therefore, we scaled it down to fit our study so that the energy consumption in the day was 45 MWh. Fig. 5 shows the load profile.

We also used the locational marginal prices (LMP) in the same day to calculate the EV charging/discharging cost [33]. Since the LMP are wholesale electricity prices, we scaled them up to RTP in a retail market. The retail electricity pricing varies from states to states and from residential to industry. In this study, we used the pricing in Saskatchewan, Canada as the reference and the flat rate for residential and small commercial customers was $\$0.1565/kWh$ [37]. The RTP was calculated as follows. Based on the electricity load and LMP, the energy cost was calculated as $energy\ cost = \sum (LMP \times load)$. The equivalent flat rate was calculated as $equivalent\ flat\ rate = \frac{energy\ cost}{\sum load}$.

The scaler can be calculated as $scaler = \frac{flat\ rate}{equivalent\ flat\ rate}$. Finally, the RTP was the LMP times the scaler, which is shown in Fig. 6. This pricing was used to calculate the EV charging/discharging cost.

Although the linearized degradation cost model was incorporated into the optimal V2G models, we use the Eq. 1 and 2 to calculate the actual degradation cost for a higher accuracy.

In this study, we assumed 20% EV penetration, which represented 100 EVs in the distribution network. Nissan leaf e-plus with a rated capacity of 62 kWh was used in the EV model and the full range was 275 km [38]. The daily driving distance was assumed as 30 km and the average daily driving time was assumed as 45 minutes, which was derived

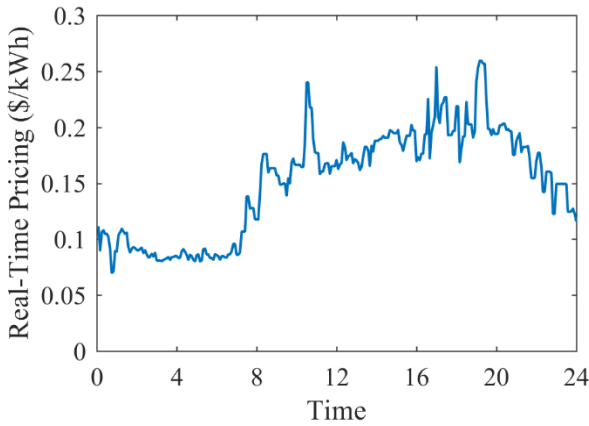


FIGURE 6. Calculated real-time pricing based on locational marginal price on October 27, 2019 in PJM market [33].

TABLE 1. Simulation parameters.

Parameter	Value
Time interval	5 minutes
Time horizon	24 hours
P_{rated} at home	1.7 kW
P_{rated} at work place	7 kW
t_1	Normal distribution with $\mu = 7:00$ and $\sigma = 1$ hour [4, 5]
t_3	Normal distribution with $\mu = 17:00$ and $\sigma = 2.8$ hours [4, 5]
a_1	0.0270
b_1	-0.0021
a_2	0.2258
b_2	-0.1411
β	0.11
SOC_0	89%
SOC_{min}	0%
SOC_{max}	100%
SOC_{acc}	50%

from [39, 40]. The energy consumption of driving 30 km represents 11% of the driving capacity, which led to an 89% of initial SOC in the Scenario #1. In the Scenario #4-#5, to ensure the EV has sufficient energy for driving at t_1 and t_3 , we used $SOC_{acc} = 50\%$. The distribution of t_1 and t_3 are assumed as normal distribution and therefore t_2 and t_4 are also normally distributed.

The EVs could be charged/discharged at home with the rated power of 1.7 kW and at work with the rated power of 7.7 kW. The time horizon was 24 hours, and the time interval was 5 minutes. The Model 1 and Model 2 were solved by CVX, a package for specifying and solving convex programs [41, 42]. The major parameters are outlined in TABLE 1.

B. SCENARIO #1: WITHOUT V2G MODEL

In this scenario, no EVs were discharged nor was EV charging controlled. In addition, no EVs was charged at workplaces.

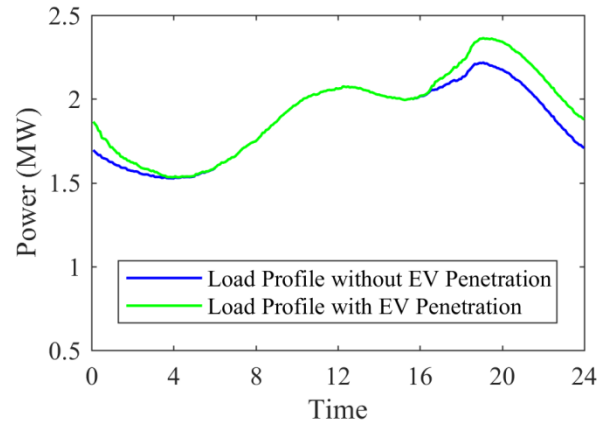


FIGURE 7. Load profiles without and with EV penetration, Scenario #1.

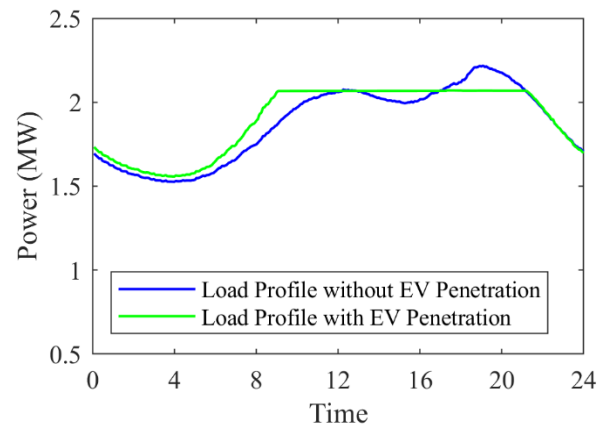


FIGURE 8. Load profiles without and with EV penetration, Scenario #2.

In other words, people arrived home, plugged in their EVs and charged up the EVs. The initial SOC was 89%.

Fig. 7 shows the simulation results in the Scenario #1. The blue line represents the load profile without EV penetration while the green line represents the load profile with 20% of EV penetration. The load profile without EV penetration is considered as the base load. The peak demand and the variance of the based load were 2.2171 MW and 0.0500 MW. The peak demand and the variance of the load profile with EV penetration were 2.3599 MW and 0.0617 MW. The charging cost of the 100 EVs was \$223 and degradation cost was \$ 28. The sum of the two costs was \$251.

The average, minimum and maximum individual EV charging cost was \$2.2287, \$1.4325, and \$2.9916 respectively. The variance of the charging cost was \$0.0980. The individual EV degradation cost was averaged at \$0.2776. The minimum and maximum degradation costs were \$0.2129 and \$0.3787.

C. SCENARIO #2: MODEL 1 WITH $\lambda = 0$

In this scenario, the Model 1 was applied to minimize the peak demand without considering the degradation cost, i.e., $\lambda = 0$. Fig. 8 shows the simulation results, in which, the blue

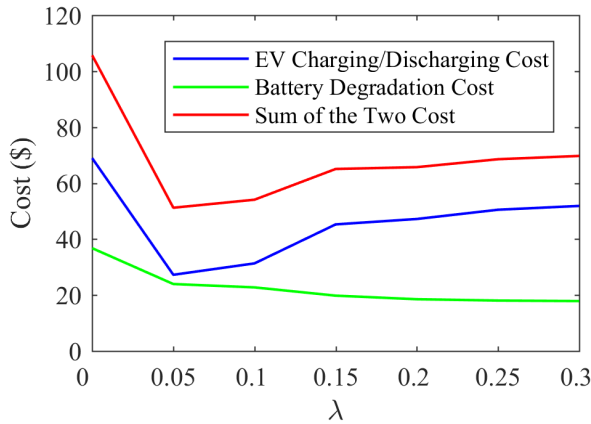


FIGURE 9. EV charging/discharging cost, battery degradation cost and the sum of the two costs of 100 EVs with respect to λ .

line represents the load profile without EV penetration while the green line represents the load profile with 20% of EV penetration.

With the proposed Model 1, the peak demand was reduced to 2.0705 MW and the variance of the load profile was reduced to 0.0403 MW. The EV charging cost was \$64 and the degradation cost was \$39. The total cost was \$103.

The average, minimum and maximum individual EV charging cost was \$0.6356, -\$1.5936, and \$1.5940 respectively. The negative cost represents that the EV owner made money. The variance of the charging cost was \$0.7009. The individual EV degradation cost was averaged at \$0.3876.

D. SCENARIO #3: MODEL 1 WITH CONSIDERATION OF DEGRADATION COST

In this scenario, the Model 1 was applied to minimize the peak demand with the consideration of the degradation cost. λ is a positive constant in this case and can play an important role in the objective function. More specifically, if λ is too small, the degradation cost function will have no effect on the overall objective function, however, if λ is too large, the degradation cost will be the dominant factor. Therefore, λ needs to be carefully chosen.

Fig. 9 shows the EV charging/discharging cost, battery degradation cost and the sum of the two with respect to a wide range of λ . As can be seen, the Model 1 with $\lambda = 0.05$ provided the minimum total cost. $\lambda = 0.05$ was then used in the objective function in this scenario.

Fig. 10 shows the load profiles without and with EV penetration. The peak demand was reduced to 2.0751 MW and the variance of the load profile with EV penetration was reduced to 0.0389 MW. The EV charging cost was \$27 and the degradation cost was \$23. The total cost was \$51.

The average individual EV charging/discharging cost was \$0.2726, the minimum was -\$0.8933, the maximum was \$0.1996, and the variance was \$0.1996. The average degradation cost was \$0.2395, the minimum was \$0.1384, the maximum was \$0.9804, and the variance was \$0.0175.

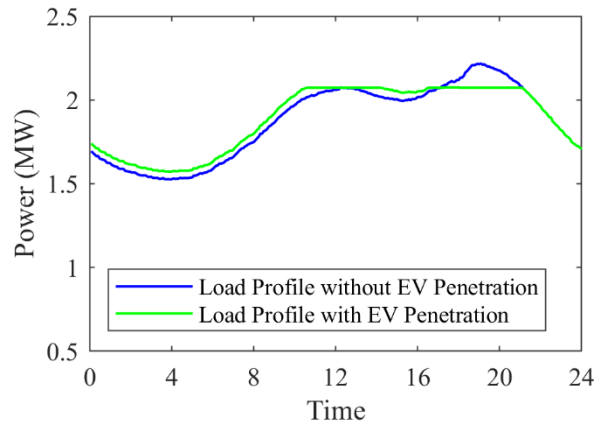


FIGURE 10. Load profiles without and with EV penetration, Scenario #3.

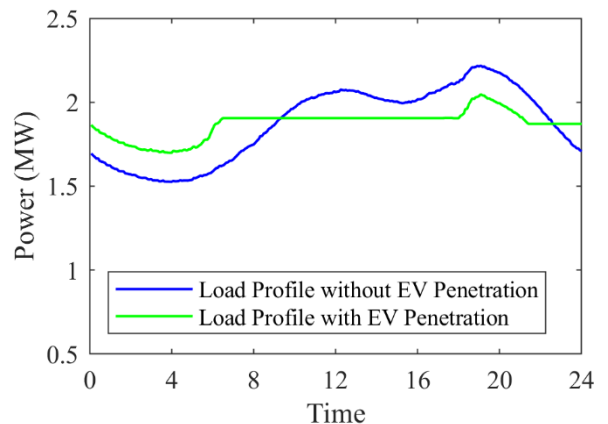


FIGURE 11. Load profiles with and without EV penetration, Scenario #4.

E. SCENARIO 4: MODEL 2 WITH $v = 0, \kappa = 0$

The Model 2 was applied with $v = 0, \kappa = 0$. Fig. 11 shows the load profiles without and with EV penetration in this scenario. With the proposed model 2, the peak demand and variance were reduced to 2.0470 MW and 0.0067 MW respectively. The EV charging/discharging cost was -\$179 and degradation cost was \$85. The total cost was -\$94. The negative cost means that the EVs create revenues.

The average EV charging cost was -\$1.7886, the minimum was -\$3.7278, the maximum was -\$0.4361, and the variance was \$0.4854. The average degradation cost was \$0.8473, the minimum was \$0.4303, the maximum was \$1.7720, and the variance was \$0.1082.

F. SCENARIO 5: MODEL 2 WITH CONSIDERATION OF DEGRADATION COST AND RTP

Similar to λ , we also quantitatively evaluated the effect of v and κ . Fig. 12 shows the EV charging/discharging cost, battery degradation cost and the sum of the two with respect to v . More specifically, the blue line shows the EV charging/discharging cost with respect to various v while the green line shows the battery degradation cost. The red line shows the sum of EV charging/discharging cost and battery

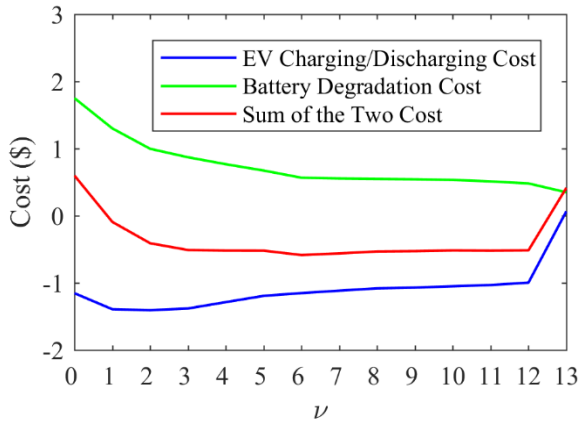


FIGURE 12. EV charging/discharging cost, battery degradation cost and the sum of the two costs with respect to ν .

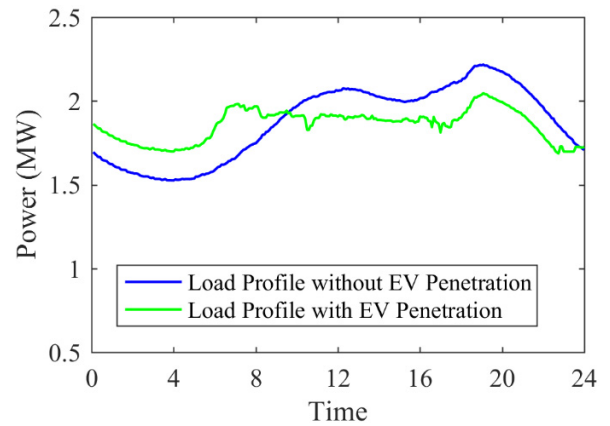


FIGURE 14. Load profiles with and without EV penetration, Scenario #5.

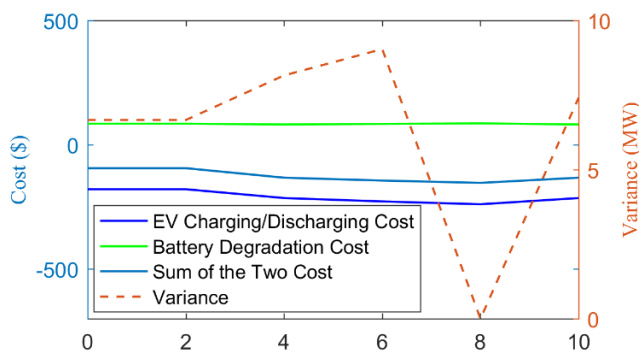


FIGURE 13. EV charging/discharging cost, battery degradation cost, the sum of the costs and the variance of the load profile with respect to κ .

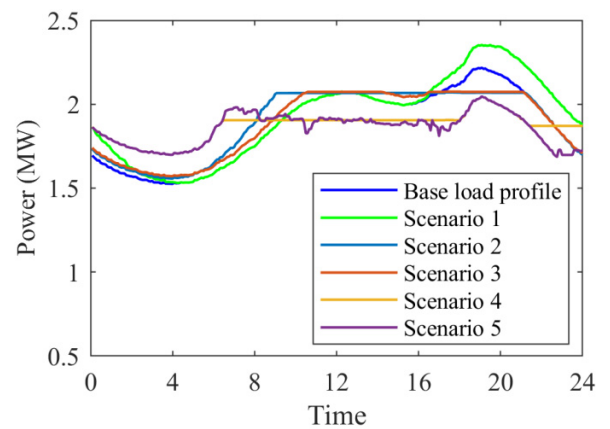


FIGURE 15. Base load profile (without EV penetration) and load profiles of Scenarios #1-5.

degradation cost. As can be seen, the sum of the costs was stable with $2 \leq \nu \leq 13$ and $\nu = 2$ was used for the Model 2 in this scenario.

Fig. 13 shows the EV charging/discharging cost, battery degradation cost, the sum of the two costs and the variance of the load profile with respect to κ .

In Fig. 13, the green line shows the battery degradation cost, which was stable with respect to κ since the ν was not changed. Both the total cost and EV charging/discharging cost decreased with increasing κ and reach the minimum at $\kappa = 8$. After that, the cost started to increase. The variance of the load profile also reached its minimum at $\kappa = 8$. Therefore, $\kappa = 8$ was selected.

Fig. 14 shows the simulation results in the application of Model 2 with $\nu = 2$ and $\kappa = 8$. The peak demand and variance were 2.0470 MW and 0.0090 MW respectively. The EV charging/discharging cost, degradation cost and the total cost were -\$239, \$86 and -\$153 respectively.

The average EV charging cost was -\$2.3930, the minimum was -\$4.2823, the maximum was -\$0.9476 and the variance was \$0.4621. The average degradation cost was \$0.8603, the minimum was \$0.4486, the maximum was \$1.5800, and the variance was \$0.0855.

IV. DISCUSSION

In this study, we have developed distributed optimal approaches to facilitate EV penetration to the power system, which minimizes multiple objectives.

Weighting factors are introduced and quantitatively evaluated to find the tradeoff among the multiple objectives. The real data including the load profile and the LMP from PJM are used to evaluate the proposed models in 5 scenarios.

The Scenario #1 is considered as the reference scenario. We consider the EV driving patterns including driving time period and driving distance, based on which, the initial SOC and required charging energy are calculated. The average daily battery degradation cost is \$0.28, which leads to a yearly degradation cost of \$102.

Fig. 15 shows the base load profile (without EV penetration) and the load profiles of the Scenarios #1-#5. Table 2 summarizes the major observations including the peak demand, the variance of load profile, the battery degradation cost, the EV charging/discharging cost and the total cost. As can be seen, with 20% of EV penetration, the uncontrolled EV charging can increase the peak demand and

TABLE 2. Summary of the major observations.

	Peak (MW) (%)	Variance (MW) (%)	Cost 1 (\$)	Cost 2 (\$)	Cost 3 (\$)
Base Load	2.2171	0.0500	-	-	-
#1	2.3599 (6.4%)	0.0617 (23.4%)	223	28	251
#2	2.0705 (-6.6%)	0.0403 (-19.4%)	64	39	103
#3	2.0751 (-6.4%)	0.0389 (-22.2%)	27	24	51
#4	2.0470 (-7.7%)	0.0067 (-86.7%)	-179	85	-94
#5	2.0470 (-7.8%)	0.0090 (-81.9%)	-239	86	-153

Note: Cost 1: EV Charging/Discharging cost; Cost 2: Battery degradation cost; Cost 3: the sum of charging/discharging and degradation cost. Negative cost means making money. % is the percentage change in comparison with the base load, in which positive numbers represent increase while negative values represent decrease.

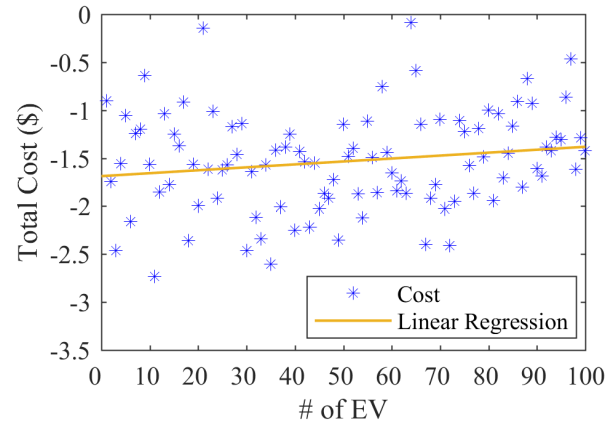
variance of the load profile by 6.4% and 23.4% respectively. Therefore, a very large number of uncontrolled EV penetration can jeopardize the power system stability.

Since the power generation cost is directly proportional to the load magnitude due to economical generation dispatch, reducing peak demand can effectively reduce the generation cost and hence the electricity prices. Therefore, the Model 1 is developed to minimize the peak demand. In addition, this approach can avoid peak demand rebound from purely minimizing electrical energy cost based on the RTP. By only minimizing peak demand in the Scenario #2, the quality of all the observations are improved. For example, the total cost is reduced from \$251 to \$103. With the consideration of the battery degradation cost, the performance is further improved. For instance, the total cost is reduced to \$51.

However, as can be seen from Fig. 15, by minimizing peak demand in the Scenario #2 and #3, the Model 1 fails to encourage EV owners to charge EVs in the off-peak demand periods.

To improve this limitation, the Model 2 is developed to minimize multiple objectives including the variance of the load profile, the battery degradation cost and the EV charging/discharging cost based on the RTP. The model performance in the Scenario #4 and #5 are significantly improved. We can see that the peak demand remains the same in both the Scenario #4 and #5. Although the battery degradation cost and the variance in the Scenario #5 are slightly higher than the Scenario #4, the total cost is dramatically reduced in the Scenario #5. Therefore, the Scenario #5 is identified as the best scenario.

In comparison with the Scenario #1 and the Scenario #5, the degradation cost is increased by 207%; however, the charging/discharging cost is reduced by 207% with a larger base value. In addition, the overall cost is reduced by 161%.

**FIGURE 16. Total cost of individual EVs. The total cost is the sum of EV charging/discharging cost and the battery degradation cost.**

In fact, the 100 EVs earns \$153 instead of paying for the electricity.

Furthermore, the weighting factors in the Model 2 are quantitatively studied and $\nu = 2$, $\kappa = 8$ provide the best performance. This provides a baseline for an EV aggregator or a utility to develop such models and design contract with EV customers.

Fig. 16 shows the total cost of individual EVs, where the markers show the cost and the line shows the linear regression. The simulation is conducted using Monto Carlo method and the # of EV is corresponding to the EV plug-time order/time. As can be seen, a later EV has a slightly higher cost. This is because the latter EVs do not have as much freedom as the earlier EVs since the total load profile changes with time. Although, this is not a significant problem because the EV plug-in time of various customers are random, this factor should be considered by a utility when the model is implemented and/or the contract is designed.

V. CONCLUSION

The increasing popularity of EVs in the transportation sector poses both opportunities and challenges to power systems. The opportunities include V2G applications for reducing peak demand, integrating intermittent renewable energy and providing ancillary services while the optimal EV charging/discharging control with consideration of battery degradation remains a great challenge.

This paper proposes optimal V2G models and a distribute control algorithm to tackle the challenges and unlock the opportunities. Case studies show that the proposed Model 2 can effectively incorporate the EV penetration to power systems by minimizing multiple objectives including the variance of load profile, the battery degradation cost and the charging/discharging cost based on RTP. More specifically, the approach can reduce the peak demand and variance of the load profile by 7.8% and 81.9%. Although the degradation cost increased from \$28 to \$86, the sum of EV charging/

discharging cost and degradation cost is decreased from \$251 to -\$153. In fact, the 100 EVs earn \$153 from the V2G program. In addition, the weighting factors of the multiple objectives are quantitatively evaluated, and the values provide a baseline for a utility or an EV aggregator to implement the proposed model.

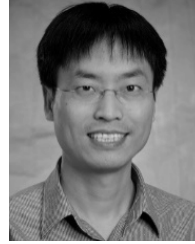
REFERENCES

- [1] K. Kaur, N. Kumar, and M. Singh, "Coordinated power control of electric vehicles for grid frequency support: MILP-based hierarchical control design," *IEEE Trans. Smart Grid*, vol. 10, no. 3, pp. 3364–3373, May 2019.
- [2] C. Liu, K. T. Chau, D. Wu, and S. Gao, "Opportunities and challenges of vehicle-to-home, vehicle-to-vehicle, and vehicle-to-grid technologies," *Proc. IEEE*, vol. 101, no. 11, pp. 2409–2427, Nov. 2013.
- [3] E. Global, "Outlook 2017. Two million and counting," Int. Energy Agency, Paris, France, Tech. Rep., 2017, doi: 10.1787/9789264278882-en.
- [4] Z. Wang and R. Paranjape, "An evaluation of electric vehicle penetration under demand response in a multi-agent based simulation," in *Proc. IEEE Elect. Power Energy Conf.*, Nov. 2014, pp. 1–6.
- [5] Z. Wang and R. Paranjape, "Optimal residential demand response for multiple heterogeneous homes with real-time price prediction in a multi-agent framework," *IEEE Trans. Smart Grid*, vol. 8, no. 3, pp. 1173–1184, May 2017.
- [6] S. Habib, M. Kamran, and U. Rashid, "Impact analysis of vehicle-to-grid technology and charging strategies of electric vehicles on distribution networks—A review," *J. Power Sources*, vol. 277, pp. 205–214, Mar. 2015.
- [7] Z. Liu, D. Wang, H. Jia, N. Djilali, and W. Zhang, "Aggregation and bidirectional charging power control of plug-in hybrid electric vehicles: Generation system adequacy analysis," *IEEE Trans. Sustain. Energy*, vol. 6, no. 2, pp. 325–335, Apr. 2015.
- [8] G. Zhang, S. T. Tan, and G. G. Wang, "Real-time smart charging of electric vehicles for demand charge reduction at non-residential sites," *IEEE Trans. Smart Grid*, vol. 9, no. 5, pp. 4027–4037, Sep. 2018.
- [9] H. Liu, J. Qi, J. Wang, P. Li, C. Li, and H. Wei, "EV dispatch control for supplementary frequency regulation considering the expectation of EV owners," *IEEE Trans. Smart Grid*, vol. 9, no. 4, pp. 3763–3772, Jul. 2018.
- [10] C. Luo, Y.-F. Huang, and V. Gupta, "Stochastic dynamic pricing for EV charging stations with renewable integration and energy storage," *IEEE Trans. Smart Grid*, vol. 9, no. 2, pp. 1494–1505, Mar. 2018.
- [11] F. Hafiz, P. Fajri, and I. Husain, "Load regulation of a smart household with PV-storage and electric vehicle by dynamic programming successive algorithm technique," in *Proc. IEEE Power Energy Soc. General Meeting (PESGM)*, Boston, MA, USA, Jul. 2016, pp. 1–6.
- [12] L. Jian, H. Xue, G. Xu, X. Zhu, D. Zhao, and Z. Y. Shao, "Regulated charging of plug-in hybrid electric vehicles for minimizing load variance in household smart microgrid," *IEEE Trans. Ind. Electron.*, vol. 60, no. 8, pp. 3218–3226, Aug. 2013.
- [13] S. Aznavi, P. Fajri, A. Asrari, and F. Harirchi, "Realistic and intelligent management of connected storage devices in future smart homes considering energy price tag," *IEEE Trans. Ind. Appl.*, to be published.
- [14] Z. Wang, R. Paranjape, Z. Chen, and K. Zeng, "A layered stochastic approach for residential demand response based on real-time pricing and incentive mechanism," *IET Gener. Transmiss. Distrib.*, early access, Nov. 2019, doi: 10.1049/iet-gtd.2019.1135.
- [15] K. Clement-Nyns, E. Haesen, and J. Driesen, "The impact of charging plug-in hybrid electric vehicles on a residential distribution grid," *IEEE Trans. Power Syst.*, vol. 25, no. 1, pp. 371–380, Feb. 2010.
- [16] J. Kang, R. Yu, X. Huang, S. Maharjan, Y. Zhang, and E. Hossain, "Enabling localized peer-to-peer electricity trading among plug-in hybrid electric vehicles using consortium blockchains," *IEEE Trans. Ind. Inf.*, vol. 13, no. 6, pp. 3154–3164, Dec. 2017.
- [17] Z. Wang, R. Paranjape, Z. Chen, and K. Zeng, "Multi-agent optimization for residential demand response under real-time pricing," *Energies*, vol. 12, no. 15, p. 2867, Jul. 2019.
- [18] L. Yao, W. H. Lim, and T. S. Tsai, "A real-time charging scheme for demand response in electric vehicle parking station," *IEEE Trans. Smart Grid*, vol. 8, no. 1, pp. 52–62, Jan. 2017.
- [19] R. Mehta, D. Srinivasan, A. M. Khambadkone, J. Yang, and A. Trivedi, "Smart charging strategies for optimal integration of plug-in electric vehicles within existing distribution system infrastructure," *IEEE Trans. Smart Grid*, vol. 9, no. 1, pp. 299–312, Jan. 2018.
- [20] H. Jiang, S. Ning, and Q. Ge, "Multi-objective optimal dispatching of microgrid with large-scale electric vehicles," *IEEE Access*, vol. 7, pp. 145880–145888, 2019.
- [21] M. Arima, L. Lin, and M. Fukui, "Three degradation parameters estimation of a LIB module using single indicator for *in-situ* charge-discharge energy prediction," in *Proc. IEEE Int. Telecommun. Energy Conf. (INTELEC)*, Oct. 2018, pp. 1–6.
- [22] Z. Wei, Y. Li, and L. Cai, "Electric vehicle charging scheme for a park-and-charge system considering battery degradation costs," *IEEE Trans. Intell. Veh.*, vol. 3, no. 3, pp. 361–373, Sep. 2018.
- [23] J. Vetter *et al.*, "Ageing mechanisms in lithium-ion batteries," *J. Power Sources*, vol. 147, nos. 1–2, pp. 269–281, 2005.
- [24] Y. Zhao, R. Fu, and S.-Y. Choe, "Modeling of SEI formation based on an electrochemical reduced order model for Li(MnNiCo)O₂/carbon polymer battery," in *Proc. IEEE Vehicle Power Propuls. Conf. (VPPC)*, Oct. 2015, pp. 1–4.
- [25] G. Ning and B. N. Popov, "Cycle life modeling of lithium-ion batteries," *J. Electrochem. Soc.*, vol. 151, no. 10, pp. A1584–A1591, 2004.
- [26] J. Christensen and J. Newman, "Effect of anode film resistance on the charge/discharge capacity of a lithium-ion battery," *J. Electrochem. Soc.*, vol. 150, no. 11, pp. A1416–A1420, 2003.
- [27] R. S. Levinson and T. H. West, "Impact of public electric vehicle charging infrastructure," *Transp. Res. D, Transp. Environ.*, vol. 64, pp. 158–177, Oct. 2018.
- [28] A. O. David and I. Al-Anbagi, "EVs for frequency regulation: Cost benefit analysis in a smart grid environment," *IET Elect. Syst. Transp.*, vol. 7, no. 4, pp. 310–317, Dec. 2017.
- [29] *A Guide to Understanding Battery Specifications*, MIT Electr. Vehicle Team, Cambridge, MA, USA, 2008.
- [30] O. Kolawole and I. Al-Anbagi, "Electric vehicles battery wear cost optimization for frequency regulation support," *IEEE Access*, vol. 7, pp. 130388–130398, 2019.
- [31] Y. Huang, "Day-ahead optimal control of PEV battery storage devices taking into account the voltage regulation of the residential power grid," *IEEE Trans. Power Syst.*, vol. 34, no. 6, pp. 4154–4167, Nov. 2019.
- [32] M. O. Badawy and Y. Sozer, "Power flow management of a grid tied PV-battery system for electric vehicles charging," *IEEE Trans. Ind. Appl.*, vol. 53, no. 2, pp. 1347–1357, Mar. 2017.
- [33] PJM. *Data Miner*. Accessed: Oct. 3, 2019. [Online]. Available: <https://www.pjm.com/markets-and-operations/tools/data-miner-2.aspx>
- [34] *What is the Average Power Usage for a Residential Customer?* BC Hydro, Vancouver, BC, Canada, 2019.
- [35] National Resources Canada. *Electricity Facts*. Accessed: Oct. 20, 2019. [Online]. Available: <https://www.nrcan.gc.ca/electricity-facts/20068#L6>
- [36] S. Wong. (2015). *Summary Report on Canadian Residential Demand Response and Ancillary Service Market Opportunities*. [Online]. Available: <https://www.nrcan.gc.ca/energy/offices-labs/canmet/publications/smart-grid/17735>
- [37] *Explaining Your Saskatchewan Electricity & Natural Gas Rates*. Accessed: Oct. 20, 2019. [Online]. Available: <https://energyrates.ca/saskatchewan/explaining-your-saskatchewan-electricity-natural-gas-rates/>
- [38] *Nissan Leaf^{e+} Battery Electric Vehicle*. Accessed: Oct. 20, 2019. [Online]. Available: <https://ev-database.org/car/1144/Nissan-Leaf-eplus>
- [39] *Journey to Work: Key Results from the 2016 Census*. Accessed: Sep. 20, 2019. [Online]. Available: <https://www150.statcan.gc.ca/n1/daily-quotidien/171129/dq171129c-eng.htm>
- [40] InsuranceHotline.com Team. *Commuting in Canada: How Your Drive To Work Stacks Up*. Accessed: Sep. 20, 2019. [Online]. Available: <https://www.insurancehotline.com/resources/commuting-in-canada-how-your-drive-to-work-stacks-up-infographic/>
- [41] M. Grant and S. Boyd, "CVX: MATLAB software for disciplined convex programming, version 2.0 beta," CVX Res., Austin, TX, USA, Tech. Rep., Sep. 2013.
- [42] M. C. Grant and S. P. Boyd, "Graph implementations for nonsmooth convex programs," in *Recent Advances in Learning and Control* (Lecture Notes in Control and Information Sciences), V. D. Blondel, S. P. Boyd, and H. Kimura, Eds. London, U.K.: Springer, 2008, pp. 95–110. [Online]. Available: http://stanford.edu/~boyd/graph_dcp.html



KENECHUKWU GINIGEME received the B.Eng. degree in electrical and electronics engineering from Madonna University, Enugu, Nigeria, in 2012. He is currently pursuing the M.Eng. degree in electronic systems engineering with the University of Regina, Regina, Canada.

His research interests include smart grid, electric vehicles, vehicle-to-grid systems, and optimization algorithms for the smart grid.



ZHANLE WANG (Member, IEEE) received the B.Eng. degree in industrial automation from the North China University of Science and Technology, Tangshan, China, in 2001, and the M.A.Sc. and Ph.D. degrees in electronic systems engineering from the University of Regina, Regina, Canada, in 2012 and 2015, respectively.

He is currently a Lecturer of electronic systems engineering with the University of Regina, Regina. His research interests focus on computational methods for power system and smart grid, including multiagent optimization, demand response, vehicle-to-grid applications, optimal dispatch of power generation, and renewable energy integration.

• • •